Journal of Thermal Analysis and Calorimetry (2019) 138:2043–2055
https://doi.org/10.1007/s10973-019-08750-3

The effect of TiO_2 particles on thermal properties of polycarbonate-based polyurethane nanocomposite films

Jelena Pavličević[1] · Milena Špírková[2] · Ayse Aroguz[3] · Mirjana Jovičić[1] · Dejan Kojić[1] · Dragan Govedarica[1] · Bojana Ikonić[1]

Received: 3 January 2019 / Accepted: 23 August 2019 / Published online: 3 September 2019

Abstract

In this work, aliphatic starting reactants were used to prepare a series of polycarbonate-based polyurethane (PC-PU) nanocomposite films with a low amount of titanium dioxide (TiO_2) nanoparticles (0.5, 1.0 and 2.0%) by one-step technique. The influence of nanoparticles on the structure and hydrogen bonding, as well as the microphase and topography of the obtained hybrid materials was followed by Fourier transform infrared spectroscopy, Atomic force microscopy and Scanning electron microscopy coupled with energy-dispersive X-ray Spectroscopy, respectively. Thermogravimetry was performed to study the effect of TiO_2 on the thermal stability and the decomposition pattern of the obtained PC-PU films. The impact of TiO_2 on the glass transition temperature, relaxation of soft domains as well as the melting of hard segments was determined by modulated differential scanning calorimetry. The significant enhancement of thermal stability and degradation of prepared hybrid materials were achieved, due to increased hydrogen bonding by addition of TiO_2. The glass transition temperatures of all PC-PU films were found independent on the titanium dioxide mass fraction. The starting of physical cross-linking disruption of the obtained hybrids was registered at significantly higher temperatures, as a consequence of the achieved interaction between uniformly dispersed TiO_2 nanoparticles and hard phase.

Keywords Polycarbonate-based polyurethane hybrid film · TiO_2 nanoparticles · hydrogen bonding · TG/DTG · MDSC

Introduction

The materials engineering science has increasingly showed a lot of interest in the possible application of nanometer scale titanium dioxide (TiO_2) across various research areas, due to its numerous advantages such as non-toxic and environmentally friendly nature, attractive physical and chemical properties, as well as satisfactory UV and weather resistance, good chemical corrosion resistance and low material cost [1–4]. Furthermore, titanium dioxide nanofillers are one of the most researched and reported materials for their multidisciplinary applications such as coatings for

✉ Bojana Ikonić
prodanic@tf.uns.ac.rs

Jelena Pavličević
jpavlicevic@uns.ac.rs

Milena Špírková
spirkova@imc.cas.cz

Ayse Aroguz
aroguz@istanbul.edu.tr

Mirjana Jovičić
jovicicmirjana@uns.ac.rs

Dejan Kojić
kojic.d@hotmail.com

Dragan Govedarica
dragang@uns.ac.rs

[1] Faculty of Technology Novi Sad, University of Novi Sad, Bulevar cara Lazara 1, Novi Sad 21000, Serbia

[2] Institute of Macromolecular Chemistry AS CR v.v.i, Heyrovského nám. 2, 162 06 Prague, Czech Republic

[3] Engineering Faculty, Istanbul University-Cerrahpasa, Avcilar Campus, Avcılar, 34320 Istanbul, Turkey

implants, drug carriers in targeted drug delivery or bio imaging [5–7].

Nowadays, polymeric nanostructured materials with improved, chemical resistance, thermal and mechanical properties of composites are of great importance for different global industrial and business sector, including medicine, pharmaceutical, electrical, furniture and packaging industry [8–10]. Accordingly, polymer hybrids containing low fraction of TiO_2 nanoparticles are very encouraging type of new materials with enhanced optical, electrical, thermal and mechanical characteristics [11]. Therefore, it is quite demanding to choose a proper preparation procedure, in order to achieve a good dispersion of nanosize inorganic filler into the polymer matrix.

As an essential class of polymer nanocomposites, thermoplastic polyurethane elastomers have been investigated in detail and used in different applications, thanks to their melt-processability and rubber-like behavior at the service temperature [12, 13]. Thermoplastic polycarbonate-based polyurethanes are widely used engineering materials as thermal protective coatings, industrial parts, building materials and footwear, as well as for tissue engineering, drug delivery system, medical equipment and implants [14–17]. These elastomers owe their excellent physical and chemical properties (biostability, biocompatibility, enhanced thermal and mechanical behavior) to the microphase segregated structure consisting of hard and soft segments [18]. The soft segments are originated from polycarbonate diol component characterized by low glass transition temperature, and, at the same time, accrediting the flexibility of polyurethanes. On the other hand, the hard domains act as physical cross-linkers, enhancing the mechanical strength and decreasing the elasticity of segmented polyurethanes properties [19, 20].

In order to improve final properties of thermoplastic polyurethanes, the utilization of different nanofillers (organoclays, Al_2O_3, SiO_2, ZnO, carbon nanotubes, etc.) has been described by now [21–26]. Recently, the use of TiO_2 nanoparticles, as effective enhancer of stability, thermal behavior and flame retardancy of polyurethanes, is reported [27–29]. However, it is necessary to pay attention to proper selection of starting components and preparation procedure condition, since TiO_2 nanofillers have a great tendency to be attracted by hydroxyl groups of polyol. For this reason, it is efficient to use a help of ultrasonication, to obtain polyurethane nanocomposites with well-dispersed titanium dioxide nanoparticles [30].

The multidisciplinary science audience is very concerned about the risk of fire due to the extensive use of polyurethane-based materials, since various applications of these materials require their utilization under the external stresses such as heat, fire, etc. [31]. Better understanding of materials behavior at high service temperatures provides proper and safety conditions for their application. The use of thermoplastic polycarbonate-based polyurethanes during hot work activities can lead to their thermal degradation (bonding breaking down), while their products may be toxic [32]. Therefore, it is very important to outline the influence of TiO_2 nanoparticles on thermal stability and decomposition of investigated materials. The compatibility of TiO_2 nanoparticles enables improved heat resistance structure in which high dielectric constant property of TiO_2 plays an important role in later degradation.

Herein, an attempt is made to study in detail the structure and hydrogen bonding of synthesized polycarbonate-based polyurethanes with low TiO_2 content, using Fourier transform infrared spectroscopy and atomic force microscopy. Thermogravimetry was carried out in nitrogen and air atmospheres. The focus is also paid to the evaluation of the titania influence on thermal properties (glass transition temperature and hard segments melting) of the obtained materials by modulated differential scanning calorimetry.

Experimental

Materials

The soft segments, deriving from the aliphatic polycarbonate diol with molecular mass of about 1000 g/mol (PCDL T4671), are agreeably provided by Asahi Kasei Chemical Corporation. PCDL T4671 diol is a telechelic linear oligomer containing hexylene (C6) and butylene (C4) units (molar ratio of C4/C6 is 3:7), connected by carbonate groups end-capped by hydroxyl groups. The detailed specification of chosen diol (OH value: 109.9 mg KOH/g; viscosity at 50 °C: 2388 mPa s, etc.) is listed in foregoing work [33]. The diisocyanate component (1,6-diisocyanatohexane), the chain extender (1,4-butanediol) and the catalyst (dibutyltin dilaurate) were supplied by Fluka Chemical Corporation. As nanofiller, hydrophilic fumed titanium(IV) oxide nanoparticles (Aeroxide TiO_2 PF2) from Evonik Industries, Germany, was used (average nominal diameter of 20 nm and specific surface area in the range of 45–70 $m^2\ g^{-1}$).

Preparation procedure

The one-step preparation procedure, used to synthesize polycarbonate-based nanocomposites, was described in details in our previous papers [33, 34]. The appropriate mass of the starting components was calculated on the basis of equal ratio of hydrogen-donor groups from the chain extender and macrodiol, respectively. 1,6-diisocyanatohexane was added in a small excess (NCO/OH_{total} = 1.05). Primary, TiO_2 nanoparticles in different mass

fraction (0.0, 0.5, 1.0 and 2.0%) were dispersed in the polycarbonate diol using magnetic stirrer for 2 h, and additionally in ultrasonic bath for 20 min. In the next step, the chain extender was added. Then, diisocyanate component was added and it was mixed. The final mixture, after being degassed, was spread on the polypropylene sheet using a ruler with a slot-width of 300 μm, and left in the oven for 24 h at 90 °C, in order to obtain polyurethane films. The codes of synthesized aliphatic polycarbonate-based polyurethanes (Table 1) are formed on the basis of the mass amount of titanium(IV) oxide (e.g., sample with no filler is marked by number 0, samples with 0.5, 1.0 and 2.0% are coded by numbers 0.5, 1 and 2, respectively).

Fourier transform infrared spectroscopy (FTIR)

The Fourier transform infrared spectroscopy (Thermo Nicolet Nexus 670 FTIR-ATR) was used to investigate the structure of obtained polyurethane hybrid materials as well as to study the influence of titanium dioxide on the hydrogen bonding index. FTIR spectra of the prepared elastomeric materials were obtained after averaging 40 scans in a transmittance mode, in the wavenumber range between 4000 and 500 cm^{-1}. The measurements were performed on three different selected areas of pure PU and the nanocomposite films, in order to obtain average values of hydrogen bonding index, HBI.

Atomic force microscopy (AFM)

Commercial atomic force microscope (Dimension Icon, Bruker) equipped with the SSS-NCL probe Super Sharp SiliconTM-SMP-Sensor (NanosensorsTMSwitzerland); spring constant 35 N m^{-1}, resonant frequency ≈ 170 kHz) was used to study the microphase-separated structure and topography of prepared polyurethane elastomeric nanocomposites. The measurements of pure PU and nanocomposite surfaces were done at ambient temperature, in the tapping mode. The surface size of obtained square scans was in the range from 1 to 2500 μm^2.

Table 1 Sample codes and the calculated hydrogen bonding index of polycarbonate-based polyurethanes filled with different content of TiO_2

Sample code	TiO_2 content/%	Hydrogen bonding index, HBI/%
0	0.0	71.4 ± 1.2
0.5	0.5	74.6 ± 1.3
1	1.0	78.0 ± 1.9
2	2.0	84.2 ± 3.8

Scanning electron microscopy coupled with energy-dispersive X-ray spectroscopy (SEM/EDX)

Samples were fixed on a metallic support using conductive silver paste (Leitsilber G302, Christine Groepl, Austria) and sputtered with platinum, in order to avoid charging and to increase the sample stability under the electron beam (Pt layer thickness 4 nm; vacuum sputter coat a secondary electron imaging (HVSEM/SE) and backscattered electron imaging (HVSEM/BSE) at 30 kV. The used detector is shown on each SEM micrograph. Backscattered electron detector shows material contrast, i.e., elements with higher atomic mass appear brighter and whiter than matrix from C, O, H elements. Each SE and BSE micrographs are taken on the exactly same place/position of the sample.

Thermogravimetric analysis (TGA)

The influence of TiO_2 nanoparticles on the thermal stability and decomposition of obtained polyurethane hybrid materials was examined using TA Instruments' Q50 TGA. The measurements were done under air and nitrogen atmospheres with a flowing rate of 50 cm^3 min^{-1}, in the temperature range from 25 to 800 °C, at the heating rate of 10 °C min^{-1}. The sample masses were about 5.0 mg.

Modulated differential scanning calorimetry (MDSC)

The investigation of the influence of TiO_2 on the thermal characteristics (glass transition temperature, the interfacial relaxation and disruption of physical cross-links) of synthesized polyurethane nanocomposite films was carried out by modulated differential scanning calorimeter (MDSC Q1000 TA Instruments). The sample masses were about 4 mg. The experiments were performed under nitrogen atmosphere, between − 80 and 180 °C, with a heating rate of 10 °C min^{-1}.

Results and discussion

The low glass transition soft segments originate from polycarbonate diol, while stiff hard domains are made of 1,6-diisocyanatohexane and chain extender (1,4-butanediol) building units.

The schematic presentation of used starting components and resulting linear thermoplastic polyurethane/TiO_2 hybrid material is given in Fig. 1, showing possible interactions between functional groups.

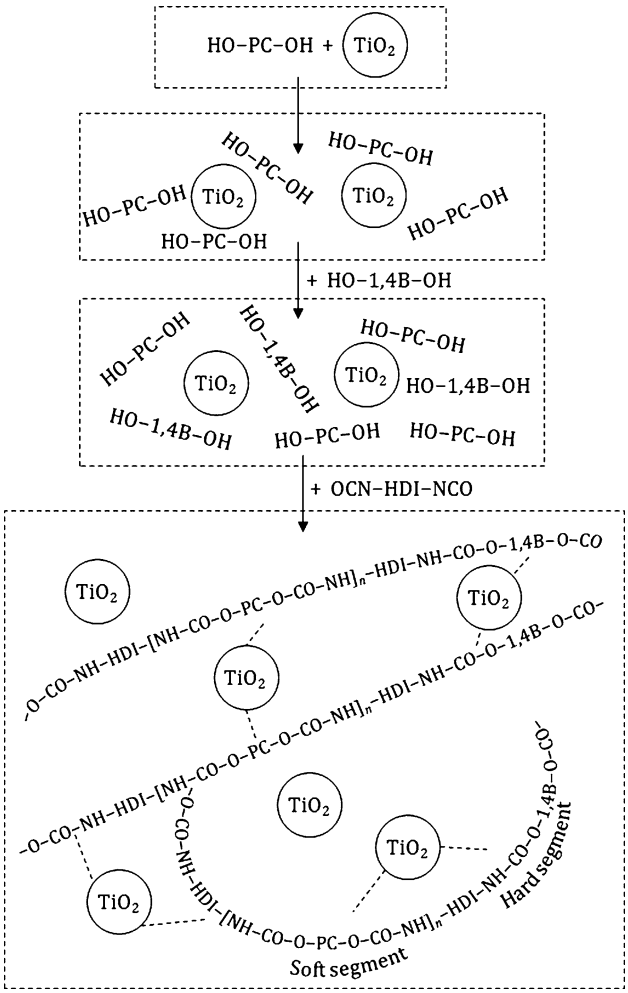

Fig. 1 The schematic illustration of starting components and the structure of polyurethane/TiO_2 nanocomposites

Material structure analysis

The influence of TiO_2 nanoparticles on the structure and hydrogen bonding formation was studied by attenuated total reflection Fourier transform infrared spectroscopy. Figure 2 shows the characteristic bands of free and hydrogen-bonded carbonyl and amine groups depending on the TiO_2 content.

The absorption region (Fig. 2a), registered between 3300 and 3350 cm^{-1}, belongs to hydrogen-bonded amine stretching groups. The increase in the peak intensity with the increasing TiO_2 loading compared to the corresponding peak in PU without TiO_2 is a confirmation of good titania dispersion that results in additional hydrogen bonding formation and the increase in the phase separation degree. CH_2 asymmetrical and symmetrical stretching, assigned to absorption peak of polycarbonate diol, were detected in the wavenumber region from 2890 to 3000 cm^{-1} (Fig. 2b). The intensity of absorption peak, registered between 1190 and 1300 cm^{-1} (Fig. 2d), and ascribed to the C–O–C asymmetrical stretching, increased by the titania presence, most probably due to the achieved interaction between the soft phase and homogeneously dispersed nanoparticles [35]. The carbonyl group region is in the wavenumber region from 1600 to 1800 cm^{-1} (Fig. 2c). Since it gives information on hydrogen bonding formation, the data are analyzed by deconvolution of the bands.

The influence of the TiO_2 nanofillers on the phase separation of the polyurethane hybrid materials was assessed by applying Gaussian deconvolution transformation of the detected carbonyl group absorbance region. Figure 3 presents an example of deconvoluted carbonyl absorbance group for the sample with 1.0% of TiO_2. The three deconvoluted carbonyl peak areas, with peak positions at 1655, 1682 and 1715 cm^{-1} and marked as 1, 2 and 3 in Fig. 3, are related to H-bonded carbonyl groups (in soft segments, in ordered hard segments and in the amorphous region, respectively). The deconvoluted C=O peak area 4, with the maximum at 1742 cm^{-1}, is ascribed to the free carbonyl group of the aliphatic carbonate.

The average value of hydrogen bonding index with standard deviation (Table 1) was determined by using Eq. (1) [36], calculating the surface area of the four deconvoluted bands in absorbance carbonyl region, obtained for three different selected areas of unfilled elastomer and PU hybrid films [36]:

$$\text{HBI, } \% = \frac{A_1 + A_2 + A_3}{A_1 + A_2 + A_3 + A_4} \cdot 100 \quad (1)$$

It can be noticed that the addition of titanium(IV) oxide fillers increased the hydrogen bonding index from 72.4% of the pristine sample to 83.5 for the elastomer containing 2.0% of TiO_2. It is supposed that positive effect of nanofiller addition on HBI values is a result of uniform distribution of titania in polyurethane matrix, confirming the absence of particles agglomeration which would cause the deterioration of hydrogen bonding.

AFM analysis of PU nanocomposites

Nanometer to micrometer surface topography and heterogeneity relief of PU-TiO_2 film surfaces were studied by AFM in the tapping mode. AFM scans covered areas from 1×1 μm^2 to 50×50 μm^2. Figures 4 and 5 show 50×50 μm^2 surface characteristics of nanocomposites with 0.0, 0.5, 1.0 and 2.0% of TiO_2. Roughness values of nanocomposites are given in Table 2.

AFM results show that PU nanocomposites differ from pure PU material in the height, but also in phase measurements. Pure PU has the smoothest surface, and it is the most homogeneous sample, while the nanocomposite with 2.0% of TiO_2 has the roughest surface.

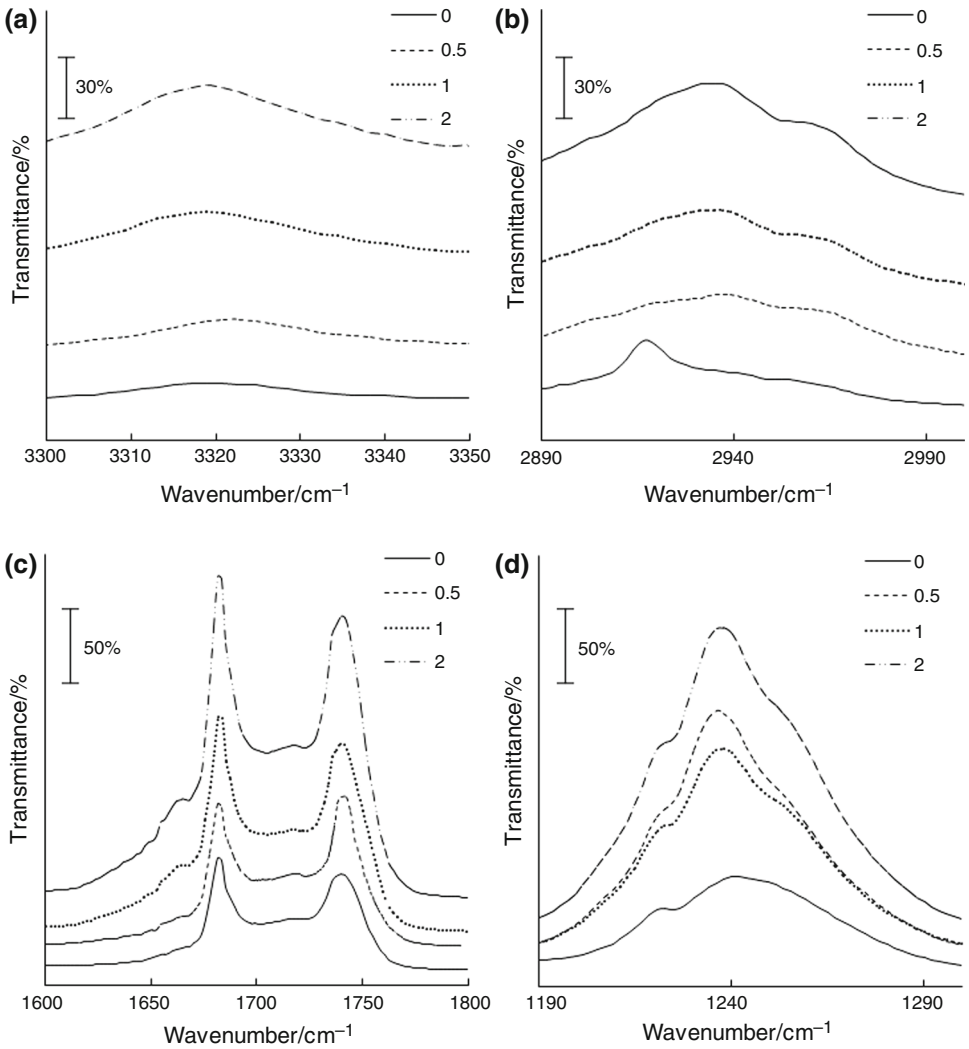

Fig. 2 FTIR absorbance band characteristics for obtained aliphatic-based polyurethanes with different titania nanoparticles loading: **a** hydrogen-bonded amine stretching groups, **b** CH_2 asymmetrical and symmetrical stretching, assigned to absorption peak of polycarbonate diol, **c** carbonyl group region and **d** C–O–C asymmetrical stretching

The sample containing 0.5% of TiO_2 is very interesting because the individual TiO_2 particles, protuding from the PU matrix, are detectable. Figure 6 shows 2D height and phase images of $10 \times 10\ \mu m^2$ area. Section analysis allowed the assessing of the size and shape of TiO_2 filler. The individual TiO_2 nanoparticles are platelets of nm order up to 1 μm size with random arrangement on the PU-TiO_2 nanocomposite surface. The size of the particles highlighted by blue ovals is about 1000×1000 nm (bottom), $1400 \times 1400\ nm^2$ (middle) and of thickness ca. 150 nm (left). However, one has to take into account that particles are covered by the layer of PU matrix. In this way, only the shape, but not the true size of pure TiO_2, is detectable (which is lower than that given by AFM).

SEM/EDX analysis of PU nanocomposites

SEM microscopy was used for the determination of surface morphology of the obtained PU nanocomposites. SEM images of polyurethane films with the lowest and the highest amount of titania, obtained using SE and BSE detectors, are shown in Fig. 7.

SEM analysis confirmed that surfaces of investigated samples are characterized by wavy relief. The brighter particles present TiO_2 fillers, while darker areas are assigned to PU matrix. The forms of aggregates are detected in SE and BSE micrographs, but well-dispersed in polyurethane films. The phase separation increases with increasing nanoparticles loading. SEM/EDX values of the polyurethane films with different content of titania nanoparticles are summarized in Table 3. Ti mapping revealed that the amount of used inorganic filler (0.5 and 2.0%) does not correspond exact to the present content of Ti elements in mass percents (0.3 and 1.4, respectively), but it can serve as accurate orientation. Platinum does not come from the samples, but from the fact that was added during sputter coating before microscopy. The obtained SEM/EDX data are in a good accordance with FTIR and AFM results.

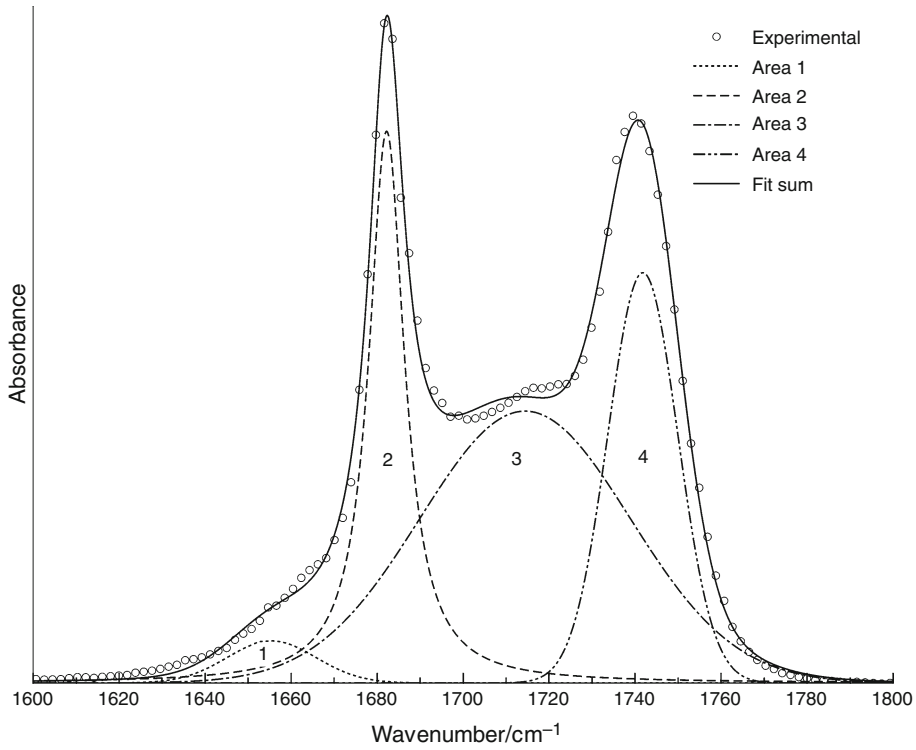

Fig. 3 Deconvoluted ATR-FTIR spectrum of C=O group absorbance region for polyurethane nanocomposite containing 1.0% of TiO_2

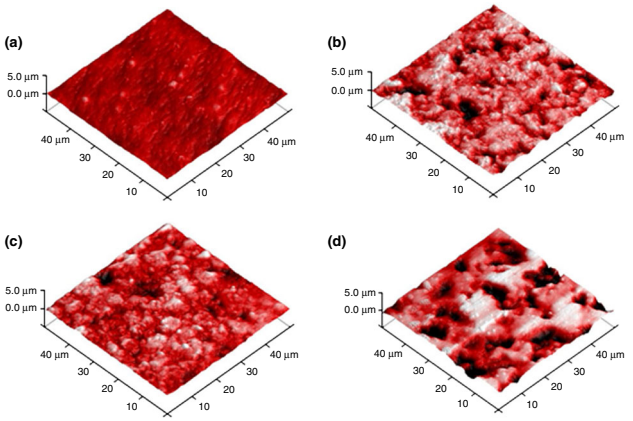

Fig. 4 AFM 3D surface height images of PU samples with: **a** 0.0%, **b** 0.5%, **c** 1.0% and **d** 2.0% of TiO_2

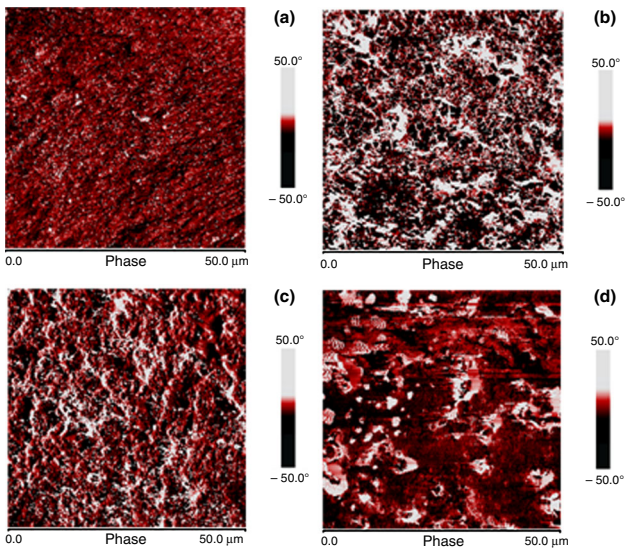

Fig. 5 AFM phase images of PU samples with: **a** 0.0%, **b** 0.5%, **c** 1.0% and **d** 2.0% of TiO_2

Thermal stability of prepared materials

TG analysis is very useful tool for the evaluation of the possible application of materials under high temperature service in different atmospheres, as it is the case of the obtained polyurethane nanocomposites, which can be potentially used as materials for the medical instruments. In this respect, it is necessary to obtain the information concerning the influence of titanium(IV) oxide nanoparticles on the thermal stability and degradation of the prepared polyurethane hybrid materials. TG curves of polyurethanes with different titania loading in the air and nitrogen atmosphere are shown in Fig. 8a, b, respectively.

TG data presented in Fig. 8 show that all samples exhibit significantly lower thermal stability in air atmosphere, which is in accordance with the expectations, since it is supposed that the oxygen presence is causing the breaking down of the polymeric chains. The small mass

Table 2 The roughness values of obtained polycarbonate-based polyurethane nanocomposites

Sample code	Surface area/μm^2	R_a^* /nm	R_q^{**} /nm	R_{max}^{***} /nm
0	2541	118	93	1024
0.5	2729	293	208	2825
1	2612	195	150	1616
2	2746	427	319	3770

Surface area: the total area of the examined sample surface

R_q^* (Rms): the standard deviation of the Z values within the given area

R_a^{**} (mean roughness): the mean value of the surface relative to the center

R_{max}^{***} (max height): the difference in height between the highest and the lowest points on the surface relative to the mean plane

Mean: the average of all Z values within the enclosed area

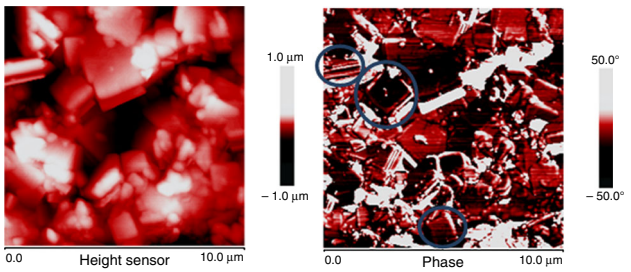

Fig. 6 AFM height (left) and phase (right) images of sample containing 0.5% of TiO_2. (objects for section analyses are highlighted by blue ovals)

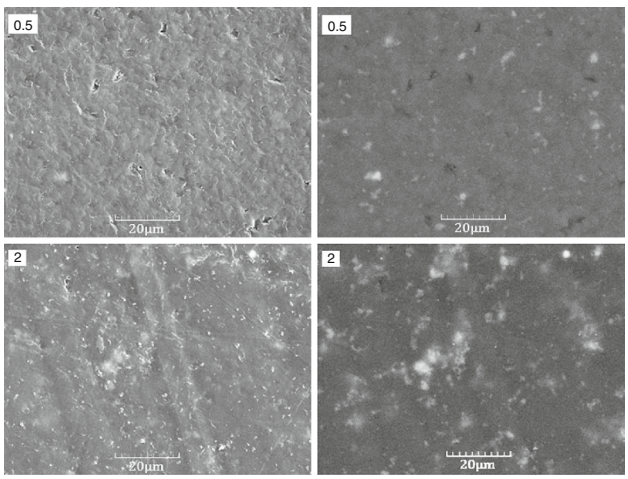

Fig. 7 SE (left) and BSE (right) micrographs of PU nanocomposites containing 0.5 and 2.0% of TiO_2. The magnification was ×2000

loss of about 2% for pristine PU, and nanocomposites is registered at 257 °C. The addition of titania increased the thermal stability of prepared elastomeric films in air atmosphere. The highest onset temperature is determined for the sample containing 2.0% of nanoparticles (312 °C). The lowest residue, determined at about 570 °C, is detected

Table 3 SEM/EDX results of PU nanocomposites containing 0.5 and 2.0% of titanium(IX) oxide

Element	Sample code			
	0.5		2	
	%	% σ	%	% σ
C	62.92	0.86	64.31	0.87
O	35.69	0.86	33.62	0.87
Ti	0.28	0.06	1.44	0.08
Pt	1.11	0.27	0.62	0.26

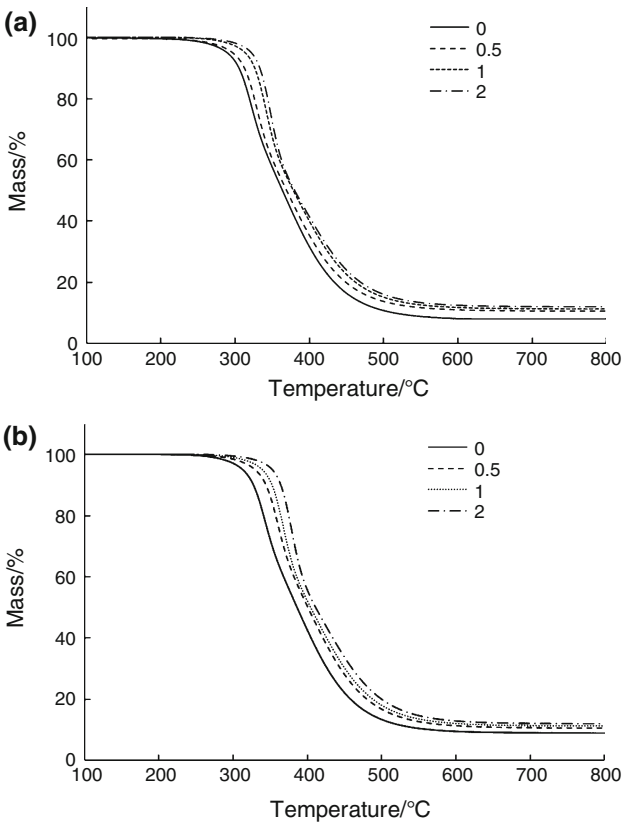

Fig. 8 Thermogravimetric curves of polycarbonate-based polyurethane nanocomposites with different titanium(IV) oxide content (0.0, 0.5, 1.0 and 2.0%) in: **a** air and **b** nitrogen atmosphere

for unfilled elastomer (5.7%), while the residue values of other nanocomposite samples were found between 7.7 and 9.2% (without observed trend in regard to TiO_2 amount). Comparing TG curves given in Fig. 8a, b, it can be also noticed that complex decomposition differs in nitrogen than in the air atmosphere.

TG data, recorded in nitrogen atmosphere, show that all samples have significantly higher thermal resistance than in air, showing thermal stability up to 285 °C, with a small mass loss of about 1.5%. The increase in titanium(IV) oxide loading significantly enhanced the thermal stability of the materials in nitrogen atmosphere, and the onset

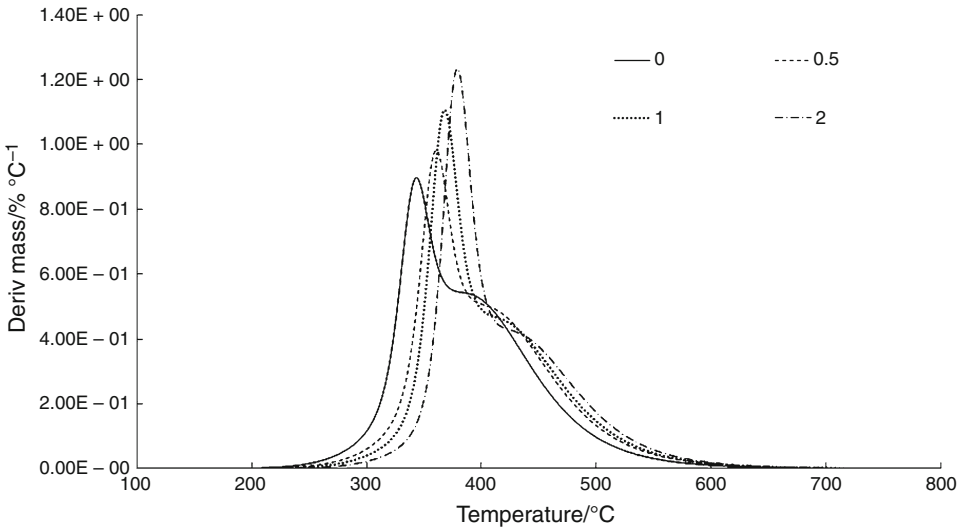

Fig. 9 DTG curves of polycarbonate-based polyurethane nanocomposites with different titania content (nitrogen atmosphere)

temperatures increase almost linearly with TiO_2 content (see Fig. 10). This increase in thermal stability with the increasing amount of the titania particles is most probably due to the ionic bonding between TiO_2 and the polymer chains, the amount of ionic cross-linking formed through fictionalization and H-bond formation [37]. The higher residue under nitrogen atmosphere was detected at higher temperatures (at 600 °C) compared to one observed in air, and it increases with the increase in titania loading from 8.9% for unfiled to 12.0% for the sample with 2.0% of titanium(IV) oxide. Since all investigated polycarbonate-based polyurethanes showed lower thermal stability in air atmosphere, the attention is aimed at detailed study of decomposition process of prepared elastomeric films in nitrogen atmosphere. The decomposition mechanism cannot be explained in detail using only data from TGA curves. However, the shape and the asymmetry in DTG curves obtained in nitrogen (Fig. 9) refer to a complex decomposition. The decomposition starts with the scission of the urethane links of the hard segments. The shoulder in DTG curves most probably belongs to the decomposition of the soft phase (polycarbonate diol) [38].

Figure 9 shows that the beginning of the onset temperature is shifted to the higher temperature region by addition of TiO_2 nanoparticles. On the other hand, the mass loss, detected for all samples at their T_{onset} values, is found to be independent on the TiO_2 content. The thermal decomposition of polyurethane/TiO_2 hybrid materials can be investigated not only on the basis of the shape of DTG curves, but also on the basis of the temperatures of the DTG peak (T_{max}) and shoulder (T_{Sh}). The increase in TiO_2 loading caused the significant shifting of DTG temperatures (from 355 °C PU with 0.5% of TiO_2 to 388 °C for the sample containing 2.0% of nanoparticles, see Fig. 9), compared to T_{max} value for pristine polyurethane sample, registered at 342 °C. This observation confirms the achieved interaction between hard segments and uniformly dispersed nanoparticles, which enabled additional hydrogen bonding formation, responsible for the enhancement of polyurethanes' thermal stability. The maximum temperature of the second degradation stage, observed as shoulder in DTG curves, is also positively affected by the titanium(IV) oxide presence. Namely, the increase in TiO_2 content caused the increase in T_{Sh} values (from 394 °C for unfilled sample to 430 °C for the samples loaded with 2.0% of nanoparticles). The detected influence of titania nanoparticles on the second DTG step (referring to the decomposition of the soft phase) indicates also the existence of the interaction between the soft domains and dispersed nanoparticles. Described DTG results support the conclusions taken on the basis of ATR-FTIR analysis (part 3.1.).

Figure 10 presents the linear increase in onset temperature, temperature of DTG peak and temperature of

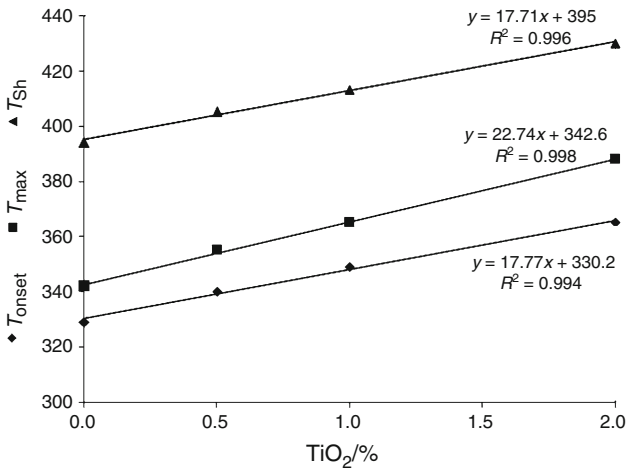

Fig. 10 The influence of TiO_2 nanoparticles on thermal stability and degradation (T_{onset}, T_{max} and T_{Sh}) in nitrogen atmosphere

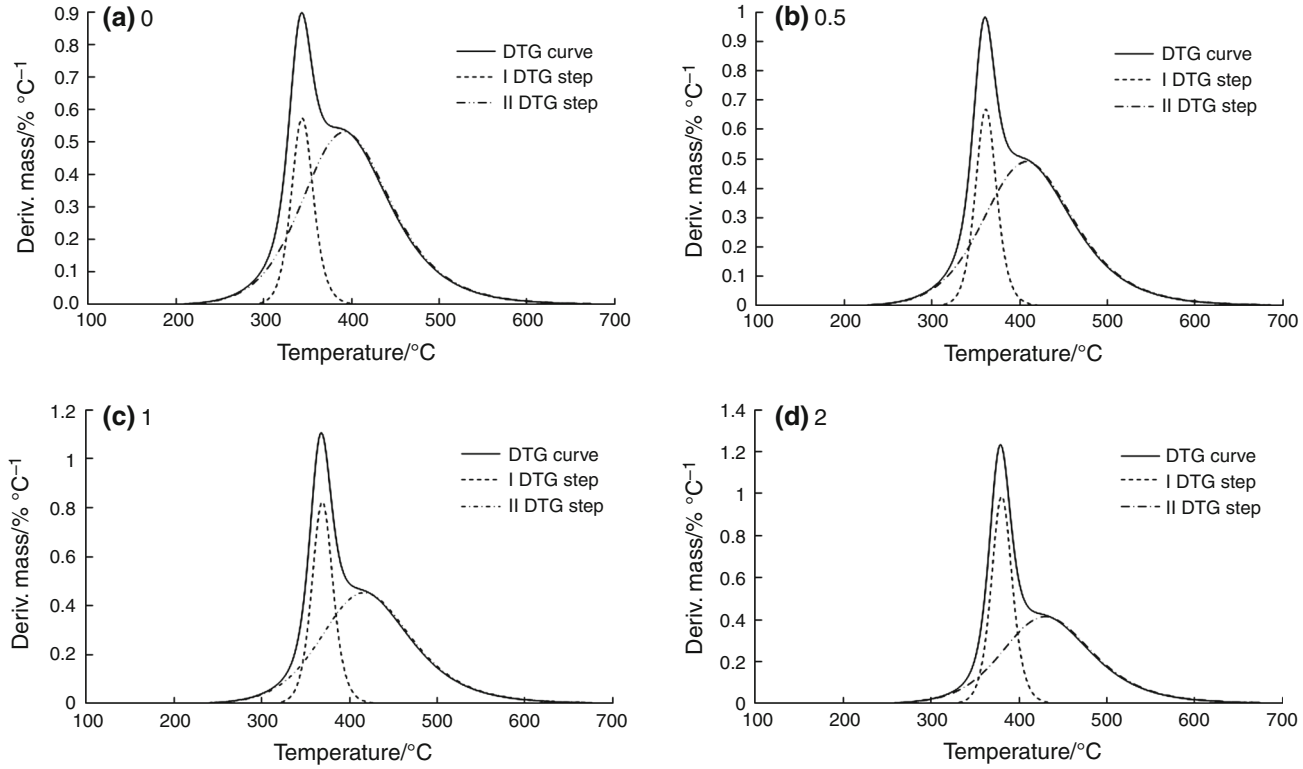

Fig. 11 Deconvolution of DTG curves of polycarbonate-based polyurethane films with different TiO_2 loading **a** 0.0%, **b** 0.5%, **c** 1.0% and **d** 2.0%

shoulder in DTG curves of polyurethane nanocomposites by increasing of titania content, in nitrogen atmosphere.

The onset temperature, temperature of DTG peak as well as temperature of shoulder in DTG curves of polyurethane nanocomposites when presented as a function of titania loading, gives a linear relationship (with high coefficient of determination, R^2 is 0.994, 0.998 and 0.996, respectively). In this way, in nitrogen atmosphere, by varying the content of nanoparticles, it is possible to predict thermal stability and degradation of polyurethane/TiO_2 hybrid materials.

Taking into account the potential application of the obtained materials under the high temperature service, DTG results demonstrate that the thermal stability in nitrogen is significantly improved by TiO_2 particles addition, and that the thermal decomposition of the polyurethane/TiO_2 nanocomposites starts at significantly higher temperatures.

In order to assess the effect of titanium(IV) oxide on the contribution of each DTG step in nitrogen atmosphere, deconvolution of the area under DTG curves obtained for polycarbonate-based films loaded with different nanofiller content was performed using Gaussian transformation (Fig. 11).

The inspection of deconvoluted DTG curves, obtained in nitrogen atmosphere, confirmed that two registered degradation processes are overlapping. Using Eq. (2) and calculating the surface areas of the first and second DTG peaks ($A_{\text{I DTG step}}$ and $A_{\text{II DTG step}}$, respectively), it is possible to determine their individual contribution to the thermal degradation process, expressed in the percentage:

$$\%_{\text{I DTG step}} = \frac{A_{\text{I DTG step}}}{A_{\text{I DTG step}} + A_{\text{II DTG step}}} \cdot 100 \quad (2)$$

The influence of TiO_2 content on the obtained values for the first thermal degradation process contribution in nitrogen is shown in Fig. 12.

It can be seen that the calculated contribution of the first DTG stage, connected to the degradation of hard domains in prepared polyurethane hybrid materials, ranges from 31.0 to 34.2%. These results are in accordance with the value of the hard segment content of the samples ($\sim$ 31%), calculated on the basis of the masses of the starting components and confirm the origin of the first degradation process.

MDSC (thermal properties)

MDSC analysis allows the separation of the reversible and the nonreversible heat flow components from the total heat flow. In this way, it is possible to distinguish kinetic changes from the thermodynamical ones, more precisely. A

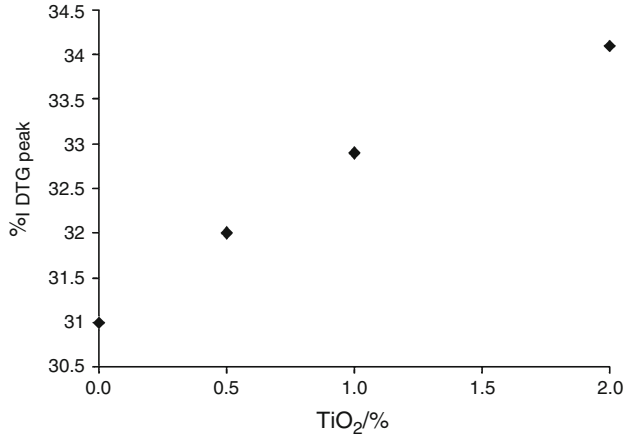

Fig. 12 The dependence of the first DTG step contribution on titania loading (nitrogen atmosphere)

typical example of MDSC experiment is shown in Fig. 13 for the sample with 1.0% of titania nanofillers.

On the basis of Fig. 13, three interesting temperature regions can be observed. The first one, detected in all curves between − 50 and − 25 °C, belongs to the glass transition region of the polycarbonate-based polyurethane elastomers. It is supposed that the second thermal event, registered only in total heat flow and nonreversible heat flow curves in the temperature range from 25 to 70 °C, is assigned to the interfacial relaxation. The absence of the change of the reversible heat flow curve in this temperature region confirms that the endothermic peak is related to the relaxation of soft segments chains in the interfacial region, as assumed [39]. The minimum temperature (registered at about 51 °C for all samples) as well as the enthalpy related to the interfacial relaxation is 0.12 J min g^{-1} $°C^{-2}$ for the pristine polyurethane and 0.18 J min g^{-1} $°C^{-2}$ for the sample containing 2.0% of nanoparticles, and they are independent of the TiO_2 content. The multiple endotherms above 100 °C in the heat flow curves are connected with the physical disruption (melting) of hard segments of elastomeric materials.

The dependence of derivative reversing heat capacity curve on the temperature for polycarbonate-based polyurethanes with different titanium(IV) oxide content is presented in Fig. 14, in order to obtain the exact value of glass transition of soft segments as well as individual hard segment melting temperatures (maxima of registered peaks above 100 °C).

The glass transition temperatures for prepared unfilled and filled polyurethane elastomers are found at about − 36 °C and are practically independent of nanoparticles content. This is in accordance with the previous results which verified that T_g value depends only on the soft segment choice. The slight shift of T_g values toward lower temperature (by about − 1 °C) was detected for the sample filled with 2.0% of titania. The small decrease in difference between T_g value of the pure polycarbonate diol (− 59 °C) and of synthesized polyurethane elastomers illustrates the slight increment of the phase separation at higher TiO_2 content (1.0 and 2.0%). The addition of TiO_2 nanoparticles did not affect significantly the surface area of the event connected with glass transition. The surface of the mentioned thermodynamic change only slightly increased with titanium(IV) oxide content (from 2.6 J min g^{-1} $°C^{-2}$, for pristine sample, to 3.0 J min g^{-1} $°C^{-2}$, for sample coded as 2).

The disruption of physical cross-linking (melting of hard segments) for unfilled sample, coded as 0, shows three peaks with maxima $T_{HS,\ m1}$, $T_{HS,\ m2}$ and $T_{HS,\ m3}$ (registered at 117, 134 and 151 °C, respectively, Table 4). The

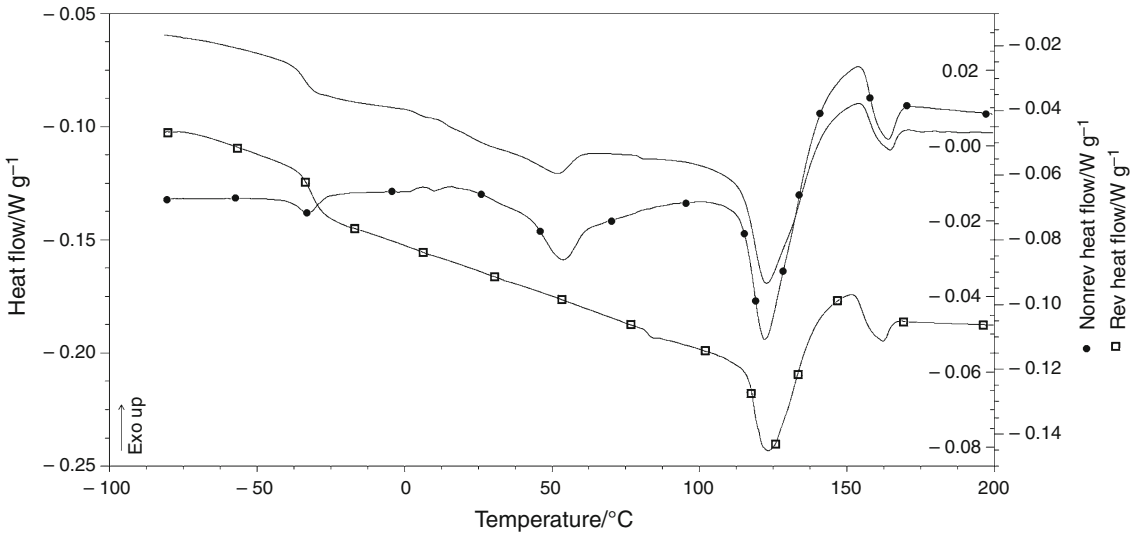

Fig. 13 Total, reversing and nonreversing heat flow versus temperature for polycarbonate-based polyurethane with 1.0% of TiO_2

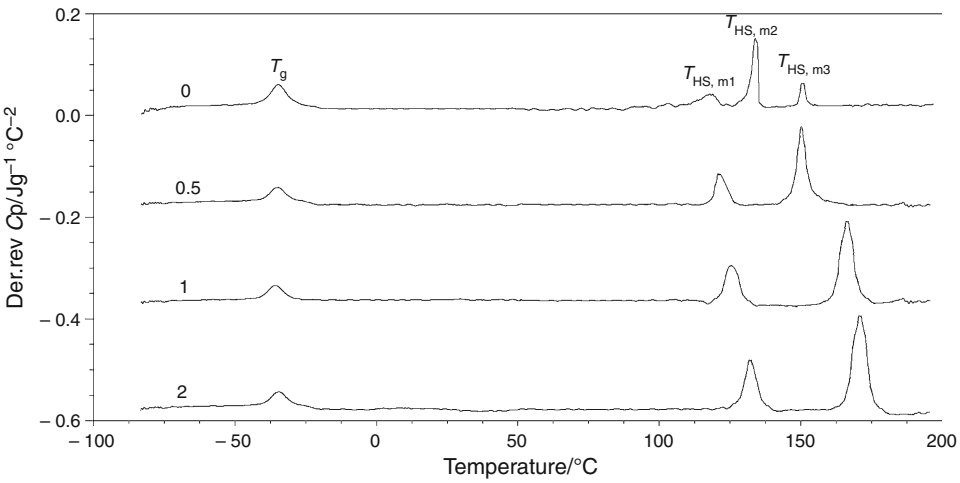

Fig. 14 Derivative reversing heat capacity curve versus temperature for polycarbonate-based polyurethanes with different TiO_2 loading

Table 4 The values of glass transition temperature and maxima peak temperatures of hard segment melting of polycarbonate-based polyurethanes with different TiO_2 content

Sample code	T_g/°C	$T_{HS, m1}$/°C	$T_{HS, m2}$/°C	$T_{HS, m3}$/°C
0	− 36	118	133	153
0.5	− 36	121	152	–
1	− 36	125	168	–
2	− 37	132	172	–

melting region of the nanocomposites is characterized with only two peaks, which appears at notably higher temperatures compared to the ones in the pristine sample ($T_{HS, m1}$, $T_{HS, m2}$ were registered at 121 and 152 °C for elastomer with 0.5% of TiO_2; at 125 and 168 °C for elastomer with 1.0% of TiO_2 and at 132 and 172 °C for elastomer with highest titania content of 2.0%). The existence of two melting peaks in derivative reversing heat capacity curve versus temperature for polycarbonate-based polyurethanes with 0.5, 1.0 and 2.0% of TiO_2 refers to more ordered hard segment domains due to the nanofiller presence and additional hydrogen bond formation, which is also confirmed by FTIR analysis. The surface area of the individual melting peaks increases with the addition of TiO_2. Moreover, the sum of the surface area of the melting peaks ($A_{HS, m}$) is significantly higher at higher titanium(IV) oxide content (Fig. 15), indicating the interaction between well-dispersed nanoparticles and hard segments.

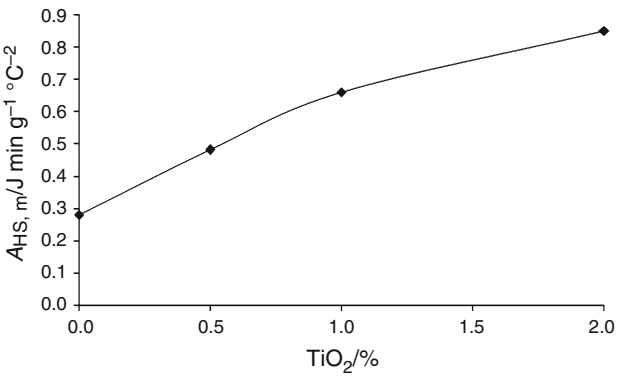

Fig. 15 The dependence of surface area of hard segment melting region on temperature for polycarbonate-based polyurethanes with different TiO_2 loading

Conclusions

Novel aliphatic polycarbonate-based polyurethane hybrid materials with low TiO_2 nanoparticles loading (0.5, 1.0 and 2.0%) were synthesized using one-step procedure. The impact of nanofiller on hydrogen bonding formation, surface topography and thermal properties of PC-PU composites was confirmed. The hydrogen-bonding-index values of prepared functional materials were increased by increment of titania, as a result of uniform distribution of nanoparticles and/or their agglomerates in polyurethane matrix (by about 11% for sample containing 2.0% of TiO_2 in regard to pure one). AFM results demonstrated that the surface roughness of PC-PU nanocomposites depends on TiO_2 loading (the roughest surface was observed for the sample with highest nanofillers mass fraction). The increase in TiO_2 has led to the formation of homogenously dispersed agglomerates detected in SE and BSE micrographs and caused higher phase separation. Ti mapping obtained by SEM/EDX analysis confirmed the amount of added inorganic nanofiller. All synthesized materials showed significantly higher thermal stability in nitrogen in regard to air atmosphere. From applicative point of view, the significant enhancement of thermal stability in nitrogen atmosphere of PC-PU materials by adding TiO_2 nanoparticles [onset temperature values of sample with 2.0% of nanoparticles mass fraction are shifted to higher value by 30 °C (from 330 to 360 °C)] was accomplished, as a

consequence of achieved ionic bonding between TiO_2 and the polymer chains. The greater residue is registered at higher temperatures in nitrogen atmosphere, and it is related to the amount of added inorganic filler. The formation of additional hydrogen bonding showed remarkably positive effect on thermal degradation of prepared hybrids in nitrogen (increasing T_{max} and T_{sh} of sample with 2.0% of TiO_2 by about 46 °C and 36 °C, respectively), which is the evidence of achieved interaction of nanofiller with both phases. The linear dependence of onset temperature and DTG temperatures on TiO_2 loading was found (with coefficients of determination higher than 0.994). The glass transition temperatures of all PC-PU materials were determined at $-$ (36 $\pm$ 1) °C, indicating the independence of T_g value on the nanoparticles content. The physical cross-linking disruption of PC-PU nanocomposites, described by two melting peaks, is registered at significantly higher temperatures. The sum of the surface area of the melting peaks increased by the rise of TiO_2 amount, confirming the interaction between well-dispersed nanoparticles/their aggregates and hard domains.

Acknowledgements The authors wish to thank for the financial supports of the Ministry of Education, Science and Technological Development of the Republic of Serbia (Project No. III45022) and of the Czech Science Foundation, Project No. 18-03932S. The authors would also like to acknowledge to Dr. Sabina Krejčíková and Dr. Magdalena Konefał from Institute of Macromolecular Chemistry AS CR in Prague for additional analyses.

References

1. Kapica-Kozar J, Piróg E, Wrobel RJ, Mozia S, Kusiak-Nejman E, Morawski AW, Narkievicz U, Michalkiewicz B. TiO_2/titanate composite nanorod obtained from various alkali solutions as CO_2 sorbents from exhaust gases. Microporous Mesoporous Mater. 2016;231:117–27.
2. Dahl M, Liu YD, Yin YD. Composite titanium dioxide nanomaterials. Chem Rev. 2014;114:9853–89.
3. da Silva VD, dos Santos JM, Subda SM, Ligabue R, Seferin M, Carone CL, Einloft S. Synthesis and characterization of polyurethane/titanium dioxide nanocomposites obtained by in situ polymerization. Polym Bull. 2013;70:1819–33.
4. Dastan D, Chaure NB. Influence of surfactants on TiO_2 nanoparticles grown by sol–gel technique. J Mater Mech Manuf. 2014;2:21–4.
5. Drnovšek N, Rade K, Milačič R, Štrancar J, Novak S. The properties of bioactive TiO_2 coatings on Ti-based implants. Surf Coat Technol. 2012;209:177–83.
6. Brammer KS, Frandsen CJ, Sungho J. TiO_2 nanotubes for bone regeneration. Trends Biotechnol. 2012;30:315–22.
7. Sawant VJ, Kupwade RV. Functionalization of TiO_2 nanoparticles and curcumin loading for enhancement of biological activity. Der Pharm Lett. 2015;7:37–44.
8. Holló BB, Ristić I, Budinski-Simendić J, Cakić S, Szilágyi IM, Szécsényi KM. Synthesis, spectroscopic and thermal characterization of new metal-containing isocyanate-based polymers. J Therm Anal Calorim. 2018;132:215–24.
9. Ristić IS, Bjelović ZD, Holló B, Szécsényi KM, Budinski-Simendić J, Lazić N, Kićanović M. Thermal stability of polyurethane materials based on castor oil as polyol component. J Therm Anal Calorim. 2012;111:1083–91.
10. Koo JH. Polymer nanocomposites. New York: McGraw-Hill, Professional Pub; 2006.
11. Wei X, Liu J. Nanocuboid TiO_2 based organic-inorganic hybrids for fast RhB trapping and photodegradation. Sol Energy Mater Sol Cells. 2016;157:139–45.
12. Oh SY, Kang MS, Knowles JC, Gong MS. Synthesis of bio-based thermoplastic polyurethane elastomers containing isosorbide and polycarbonate diol and their biocompatible properties. J Biomater Appl. 2015;30:327–64.
13. Špírková M, Machová L, Kobera L, Brus J, Poręba R, Serkis M, Zhigunov A. Multiscale approach to the morphology, structure, and segmental dynamics of complex degradable aliphatic polyurethanes. J Appl Polym Sci. 2015;132:41590–601.
14. Cipriani E, Bracco P, Kurtz SM, Costa L, Zanetti M. In-vivo degradation of poly (carbonate-urethane) based spine implants. Polym Degrad Stab. 2013;98:1225–35.
15. Osman AF, Edwards GA, Schiller TL, Andriani Y, Jack KS, Isabel C, Morrow IC, Peter J, Halley PJ, Darren J, Martin DJ. Structure–property relationships in biomedical thermoplastic polyurethane nanocomposites. Macromolecules. 2011;45:198–210.
16. Chen QZ, Liang LZ, Thouas GA. Elastomeric biomaterials for tissue engineering. Prog Polym Sci. 2013;38:584–671.
17. Fernández-d'Arlas B, Alonso-Varona A, Palomares T, Corcuera MA, Eceiza A. Studies on the morphology, properties and biocompatibility of aliphatic diisocyanate-polycarbonate polyurethanes. Polym Degrad Stab. 2015;122:153–60.
18. Fernández-d Arlas B, González I, Eceiza A. Hacia la mímesis de la seda de araña a partir de poliuretanos con segmentos cortos de unidades rígidas y semiflexibles. Rev Lat Am Metal Mater. 2015;35:39–48.
19. Mothé CG, de Araujo CR, Wang SH. Thermal and mechanical characteristics of polyurethane/curaua fiber composites. J Therm Anal Calorim. 2009;95:181–5.
20. Klinedinst DB, Yilgör I, Yilgör E, Zhang M, Wilkes GL. The effect of varying soft and hard segment length on the structure–property relationships of segmented polyurethanes based on a linear symmetric diisocyanate, 1, 4-butanediol and PTMO soft segments. Polymer. 2012;53:5358–66.
21. Sheng D, Tan J, Liu X, Wang P, Yang Y. Effect of organoclay with various organic modifiers on the morphological, mechanical, and gas barrier properties of thermoplastic polyurethane/organoclay nanocomposites. J Mater Sci. 2011;46:6508–17.
22. Pavličević J, Špírková M, Jovičić M, Bera O, Poręba R, Budinski-Simendić J. The structure and thermal properties of novel polyurethane/organoclay nanocomposites obtained by pre-polymerization. Compos Part B Eng. 2013;45:232–8.
23. Kim KT, Dao TD, Jeong HM, Anjanapura RV, Aminabhavi TM. Graphene coated with alumina and its utilization as a thermal conductivity enhancer for alumina sphere/thermoplastic polyurethane composite. Mater Chem Phys. 2015;153:291–300.
24. Kathalewar M, Sabnis A, Waghoo G. Effect of incorporation of surface treated zinc oxide on non-isocyanate polyurethane based nano-composite coatings. Prog Org Coat. 2013;76:1215–29.
25. Pavličević J, Špírková M, Bera O, Jovičić M, Pilić B, Baloš S, Budinski-Simendić J. The influence of ZnO nanoparticles on thermal and mechanical behavior of polycarbonate-based polyurethane composites. Compos Part B Eng. 2014;60:673–9.
26. Špírková M, Duszová A, Poręba R, Kredatusová J, Bureš R, Fáberová M, Šlouf M. Thermoplastic polybutadiene-based polyurethane/carbon nanofiber composites. Compos Part B Eng. 2014;67:434–40.

27. Reid DL, Draper R, Richardson D, Demko A, Allen T, Petersen EL, Seal S. In situ synthesis of polyurethane–TiO_2 nanocomposite and performance in solid propellants. J Mater Chem A. 2014;2:2313–22.
28. Chen C, Wu W, Xu WZ, Charpentier PA. The effect of silica thickness on nano TiO_2 particles for functional polyurethane nanocomposites. Nanotechnology. 2017;28:115709–23.
29. Chen X, Wang W, Li S, Qian Y, Jiao C. Synthesis of TPU/TiO_2 nanocomposites by molten blending method. J Therm Anal Calorim. 2018;132:793–803.
30. Zebarjad SM, Sajjadi SA, Raoofian I. Effect of nano size TiO_2 on morphology of polyurethane/TiO_2 nanocomposites. In: 2nd international conference on nanomechanics and nanocomposites, 10–13 Oct 2010, Beijing; 2010
31. Bikiaris D. Can nanoparticles really enhance thermal stability of polymers? Part II: an overview on thermal decomposition of polycondensation polymers. Thermochim Acta. 2011;523:25–45.
32. Shufen L, Zhi J, Kaijun Y, Shuqin Y, Chow WK. Studies on the thermal behavior of polyurethanes. Polym Plast Technol Eng. 2006;45:95–108.
33. Špírková M, Pavličević J, Strachota A, Poręba R, Bera O, Kaprálková L, Baldrian J, Šlouf M, Lazić N, Budinski-Simendić J. Novel polycarbonate-based polyurethane elastomers: composition–property relationship. Eur Polym J. 2011;47:959–72.
34. Špírková M, Poręba R, Pavličević J, Kobera L, Baldrian J, Pekárek M. Aliphatic polycarbonate-based polyurethane elastomers and nanocomposites. I. The influence of hard-segment content and macrodiol-constitution on bottom-up self-assembly. J Appl Polym Sci. 2012;126:1016–30.
35. Polizos G, Tuncer E, Agapov AL, Stevens D, Sokolov AP, Kidder MK, Jacobs JD, Koerner H, Vaia RA, More KL, Sauers I. Effect of polymer–nanoparticle interactions on the glass transition dynamics and the conductivity mechanism in polyurethane titanium dioxide nanocomposites. Polymer. 2012;53:595–603.
36. Seymour RW, Estes GM, Cooper SL. Infrared studies of segmented polyurethan elastomers. I. Hydrogen bonding. Macromolecules. 1970;3:579–83.
37. Bajsić Govorčin E, Rek V. Thermal stability of polyurethane elastomers before and after UV irradiation. J Appl Polym Sci. 2001;79:864–73.
38. Poręba R, Špirková M, Pavličević J, Budinski-Simendić J, Szécsényi M, Holló B. Aliphatic polycarbonate-based polyurethane nanostructured materials. The influence of the composition on thermal stability and degradation. Compos Part B Eng. 2014;58:496–501.
39. Poręba R, Špírková M, Brožová L, Lazić N, Pavličević J, Strachota A. Aliphatic polycarbonate-based polyurethane elastomers and nanocomposites. II. Mechanical, thermal, and gas transport properties. J Appl Polym Sci. 2013;127:329–41.